

"Smart" Packaging of Self-Identifying and Localizable mmID for Digital Twinning and Metaverse Temperature Sensing Applications

Charles A. Lynch III, Ajibayo O. Adeyeye, Manos M. Tentzeris
School of ECE
Georgia Institute of Technology
Atlanta, GA 30332-250, USA
clynch19@gatech.edu

Abstract—With the increasing demand for scalable and high performing wireless devices for Digital Twinning applications in industrial systems and in the Metaverse, there is likewise increasing demand to explore means of "Smart" packaging enabled devices. In this effort, the authors report a minimalistic, ultra-low-cost mmID module operating in the 60 GHz with a resistive-based temperature sensor for localized sensing applications. The presented system is capable of simultaneously sensing the local temperature of the self-identifying mmID while maintaining a ranging accuracy of 5.35 mm. In addition, simultaneous multi-tag interrogation capability is demonstrated through the "Smart" packaging of the mmID enabled through Frequency Division Multiplexing. Thus, the system features a framework for future Digital Twinning and Metaverse applications that utilize multiple self-identifying mmID's for localized sensing.

Keywords—mmID, Localized Sensing, Digital Twinning, Additive Manufacturing

I. INTRODUCTION

With recent advances of wireless and 5G/mm-Wave technologies, there is a realistic promise of real-world digital twinning of physical structures for data-driven, optimized operation of industrial systems. With these wireless systems expected to support over 75 billion devices by 2025, the sensor nodes of these systems need to be low-cost and highly scalable to meet the demand of these industrial systems. One choice of wireless sensor node for these systems is Radio Frequency Identification (RFID). These sensor nodes operate through encoding information on a backscattered waveform and hinge on the reader complexity to decode and monitor this information of the environment in order to digital twin an systems. These ultra-low-cost RFID systems have been utilized to wirelessly monitor local temperature, relative humidity, and gas concentration [1]–[3]. Commercially available RFID systems operate primarily in the Ultra-High Frequency (UHF) spectrum, but due to the inherent lack of bandwidth availability of this frequency range, these systems suffer in terms of precise localizable sensing applications for digital twinning of physical environments. Thus, a natural solution would be to utilize millimeter-wave Identification (mmID) technology instead and in particular with the recently updated specifications

around the 60 GHz frequency band, with an available 7 GHz of bandwidth resource, localized systems applications at this frequency band have become very appealing. Indeed, ranging accuracy within 5 mm has been reported [4] utilizing a 60 GHz system. In addition to the frequency of operation, the manufacturing approach of these backscattering mmID's needs to be highly-scalable to meet the demand of future digital twinning systems. A highly favorable solution is to package and realize these sensor nodes through Additively Manufactured technologies. This choice of fabrication provides a sustainable, low-cost solution by reducing wasted material while enabling a multitude of form-factors in order to meet application-specific needs. There have been multiple works highlighting the design and fabrication of Additively Manufactured wireless devices utilizing 3D-printing or inkjet printing fabrication techniques to enable high-performing wireless modules at mm-Wave [2], [5], [6].

Thus, the authors propose an integrated, self-identifying temperature sensing mmID tag realized through highly-scalable Additively Manufacturing Technologies. The remainder of the paper is structured as follows: In Section II, the designs of the front-end, sensing element, and baseband circuitry are described. In Section III, details of the "Smart" packaging of the mmID through Additively Manufactured mmID is presented. In section IV, the system is evaluated in both ranging and temperature sensing capabilities of the mmID system. In Section IV, multi-tag interrogation is demonstrated displaying a proof-of-concept digital twinning of the measurement scenarios that were evaluated. Finally, in Section V, the authors draw conclusions on the presented system.

II. SELF-IDENTIFYING DIGITAL TWINNING MMID SYSTEM

The self-identifying digital twinning mmID is made up of three sub components namely, the RF Front-end to communicate the ID and local temperature of the mmID, the temperature sensing element for capture fluctuations in local temperature, and the baseband circuitry in order to map the sensor response. This proof-of-concept self-identifying mmID was realized with Additively Manufacturing pack-

aging approaches in order to provide an low-cost, highly scalable mmID system for digital twinning applications.

A. RF Front-end of mmID

For any RFID/mmID sensor node, there are two main subsystems that enable backscatter communication, namely the antenna element and modulating impedance. The antenna element used in this proof-of-concept, self-identifying temperature sensor is a series-fed 4×1 linear patch antenna array. The antenna array was designed on a 0.24 mm thick poly-carbonate a flexible substrate with a $\tan(\delta) = 0.004$ providing a flexible substrate with acceptable loss and a schematic of the designed sample with dimensions of the designed array and radial stub for the modulating load impedance is displayed in Figure 1. A plot of the measured

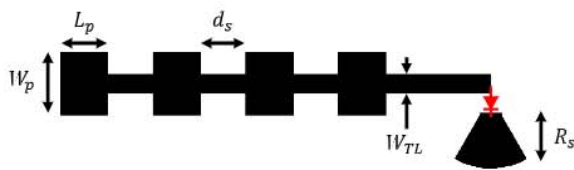


Figure 1: Schematic of the RF Front-end of the 60 GHz mmID with $W_p = 1.87$ mm, $L_p = 1.42$ mm, $d_s = 1.31$ mm, $W_{TL} = 0.59$ mm, and $R_s = 1.62$ mm.

return loss (S_{11}) of the antenna is displayed in Figure 2. With a -10 dB matching covering a frequency range of 60 GHz to 64 GHz, the operational bandwidth of the IWR6483AOPEVM radar module from Texas Instrument used to interrogate the mmID. Thus, establishing adequate performance for this self-identifying temperature sensing system. The second component of the RF front-end is the

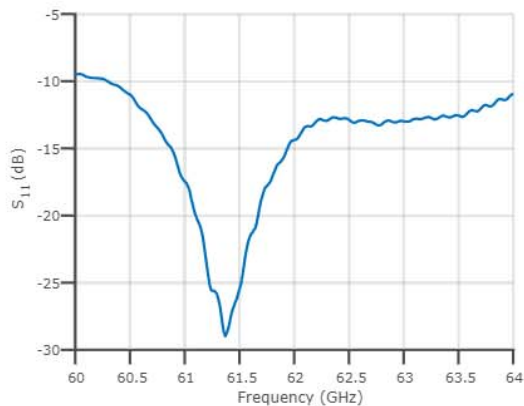


Figure 2: Measured S_{11} of 4×1 patch antenna array of mmID.

modulating load enabling encoding of the ID and the sensing information of the mmID. A phase-based modulation technique was utilized in order to provide sufficient sub-carrier generation. The modulating load consists of a diode

connected in series with a quarter wavelength radial stub such that in the zero bias condition the antenna sees an open circuit and in the biased condition, a short circuit. This yields a desired phase differential of 180° . The measured input impedance phase was characterized and displayed in Figure 3 and highlights that an adequate phase differential is observed over the entire band of operation of the reader.

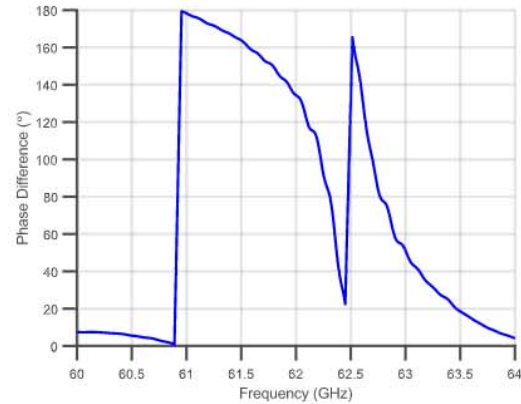


Figure 3: Phase difference of mmID load for bias of 0 V and 0.8 V for phase-based modulation.

B. Sensing Element

For the sensing element, an inkjet printed resistance-based temperature sensor was designed and characterized. Figure 4 displays the designed resistive sensor and with a total footprint of $2.89 \text{ cm} \times 1.0 \text{ cm}$, the resistive sensor displays a compact, flexible form-factor. The width of the traces of the sensor are 0.1 mm and the length of the turns are 0.54 mm. This Additively Manufactured temperature sensor was characterized from 23°C to 90°C and a plot of the resistance in Ω is displayed in Figure 5. With an estimated sensitivity of $0.0726 \frac{\% \Delta R}{^\circ\text{C}}$, the sensor presents adequate performance to enable local temperature monitoring through mmID interrogation over a wide range of temperatures.

C. Baseband Circuitry for Self-Identification

The baseband circuitry in an mmID plays a key role in the self-identifiable package and encoding the change in local temperature that the mmID experiences. A similar baseband design as [4] is employed with a wheatstone bridge circuit, a ultra-low-power operational amplifier TSU101 to amplify the sensor response, a voltage controlled oscillator (VCO) LTC6907 to provide the "ID" of the mmID, and two bias resistors that act as a voltage divider to provide the appropriate bias voltage to the schottky diode for backscattering. By utilizing this baseband circuitry design, the system can easily multiplex tags in the field-of-view (FoV) through frequency division multiplexing (FDM), or each tag having a unique baseline modulation frequency at ambient temperature. A

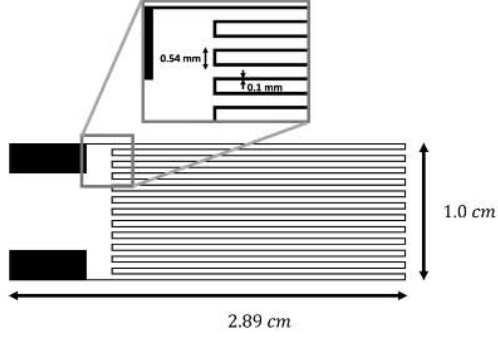


Figure 4: Schematic of the inkjet printed resistive-based temperature sensor with total footprint of 2.89 cm \times 1.0 cm.

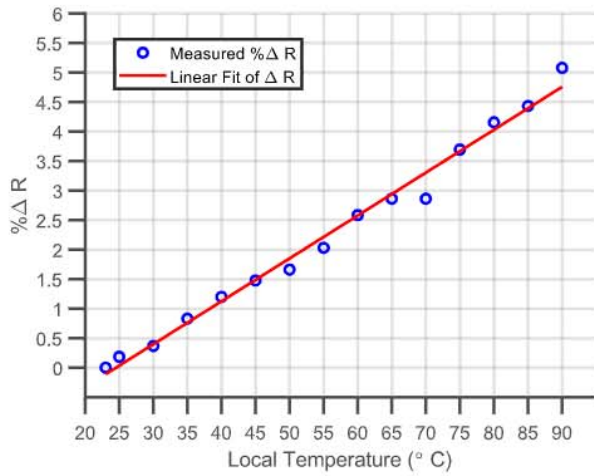


Figure 5: % ΔR vs. temperature of resistive based sensor.

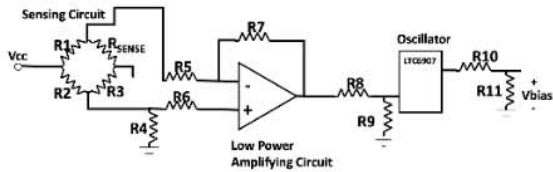


Figure 6: Baseband circuit schematic enabling sensing and self-identification of mmID.

schematic of this sensing baseband circuit is displayed in Figure 6. The major benefit of this integration and encoding scheme is the removal of a micro-controller unit which would increase power consumption and size of the mmID. The wheatstone bridge circuit and amplifier was configured to produce an output voltage difference of 0 V to 0.158 V for a single tag, but can easily be adjusted to enable FDM of multiple tags in the FoV by adjusting the bridge resistors and the gain of the differential amplifier circuitry. The oscillation frequency of the mmID was characterized

in order to map the resistance change of the temperature sensor with the Tektronix DPO 7454 Oscilloscope. The characterized modulation frequency versus local temperature of the resistive-based sensor is displayed in Figure 7 with an estimated sensitivity of 8.97 $\frac{\text{kHz}}{^\circ\text{C}}$.

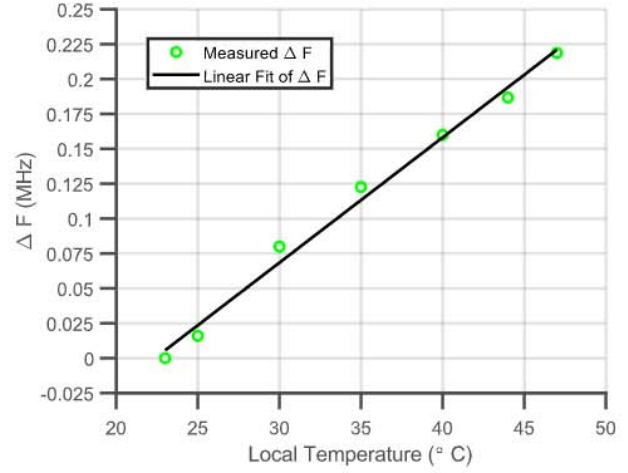


Figure 7: Modulation Frequency mmID versus the local temperature of the sensor.

III. "SMART" PACKAGING OF MMID

Having designed and characterized the sub-components of the mmID, the components were then combined with Additively Manufacturing techniques to provide a "Smart" packaging of Digital Twinning mmID sensing system. Due to the architecture of the baseband circuitry, the "ID" can be set by selecting different voltage ratios of the wheatstone bridge circuit. Thus, the functionality of the wheatstone bridge circuit is two-fold. The bridge circuit sets the baseline modulation frequency under ambient temperature conditions by setting the amplified output voltage of the differential amplifier to control the VCO. The combination of the wheatstone bridge circuit and differential amplifier maps the change in sensor impedance to local temperature of the mmID with this change in frequency providing the wireless sensing mechanism. By adjusting the R_1 R_2 , the baseline voltage ratio between the two branches of the bridge circuit is reconfigurable. Thus, the baseline frequency, and therefore, "ID" of the mmID becomes reconfigurable as well. This is crucial for multi-tag interrogation as in order to discriminate between mmIDs in the FoV of the radar, Frequency Division Multiplexing is required. Thus, providing an easily configurable "Smart" packaging for a highly-scalable multi-tag interrogation in Digital Twinning systems. Additionally, with the elimination of an MCU, an integrated, self-identifying mmID can be fully printed on a single substrate, providing compact, sticker-like, conformal form-factor. Thus, through these Additively Manufacturing processes were utilized for

the realization of the self-identifying mmID temperature sensor node. As aforementioned, these processes reduce waste and provide a highly scalable solution for the realization of "Smart" packaging devices. Prior to inkjet printing on the flexible polycarbonate substrate, the piece of polycarbonate was subject to UV ozone treatment for 1 min to improve surface wettability of the substrate and to remove organic impurities on the surface. Then the pattern of the array and sensor element was printed using the Dimatix DMP-2831 inkjet printer and the silvernano-particle ink EMD5730 from Sun Chemical. Two layers of ink were printed for the temperature sensing element and three layers of SNPs were used for the RF front-end to maintain a minimum thickness based on the skin-depth required at 60 GHz. The substrate was then sintered for one hour @ 120 °C. The diode in the RF front-end was electrically connected with a conductive silver paste which also acts as an adhesion method. Both the fabricated resistive-based temperature sensor and integrated mmID front-end can be viewed in Figure 8 and Figure 9, respectively.

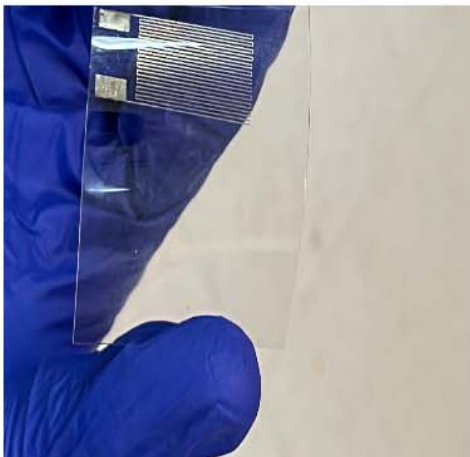


Figure 8: Flexible, inkjet resistive-based temperature sensor for digital twinning applications.

IV. SYSTEM EVALUATION

Having integrated the inkjet printed front-end, sensing element, and baseband circuitry, the "smart" packaged mmID with self-identifying and sensing capabilities was evaluated in terms of local temperature sensing and its capability for multi-tag interrogation and sensing. As aforementioned, the reader chosen for these experiments was the IWR6843AOPEVM. This small-form factor, Antenna-on-Package (AoP) radar module is displayed in Figure 10. The layout of the receiving antennas elements enables a $\pm 120^\circ$ field-of-view with each antenna element having 6 of gain. Additionally, with a rated maximum transmitted power of 12, this module enables an ultra-low-cost solution for mm-Wave sensing applications. The interrogator is operated based



Figure 9: Flexible, inkjet printed RF Front-end of mmID tag.

on the well-known Frequency Modulated Continuous Wave (FMCW) radar principles. FMCW radar involves the transmission of a chirp signal and subsequent mixing of delayed chirps that return after reflection from a series of targets in the FoV of the interrogator. The chirp parameters of each evaluation are displayed in Table I where Bandwidth is the difference between the maximum and minimum frequency of the chirp and slope is the rate of change of frequency of the chirp signal. The raw complex time domain data was sampled using the DCA1000 and mmWaveBoost evaluation boards provided by Texas Instruments. The sampled data was saved and imported into MATLAB for post-processing. Utilizing a similar signal processing method, detailed in [7], the estimation of the range and Angle-of-Arrival (AoA) was done to provide 2D localization of each self-identifying, temperature sensing mmID.

Table I: Chirp parameters used to acquire the reported measurements.

Parameter	Value
Bandwidth	3.80 GHz
Slope	24.985 MHz/ μ s
Sampling Rate	10 MHz
Chirps per Frame	120
Chirp Periodicity	160 μ s

A. Local Temperature Monitoring

For local temperature monitoring, a single mmID sensor was positioned at the ranges of 0.15 m to 0.40 m in steps of 5 cm ranges from the reader with a heat lamp at 25 cm acting as the local source of heat. The measurement setup for this evaluation is shown in Fig. 11. As explained in section II-C, the instantaneous modulation frequency of the tag is linearly mapped to the local temperature surrounding the tag. A similar ranging extraction as [4] was conducted at

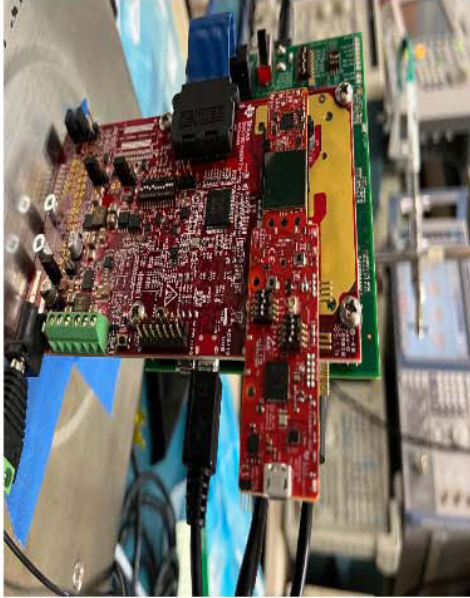


Figure 10: Ultra-low-cost FMCW radar, mounted on the DCA1000 and mmWaveBoost IC for system evaluation.

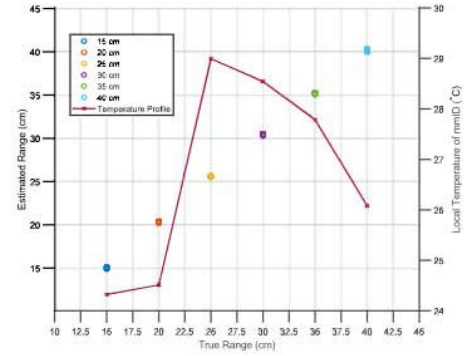


Figure 12: Estimated range and local temperature of the mmID as it passes the heat source.

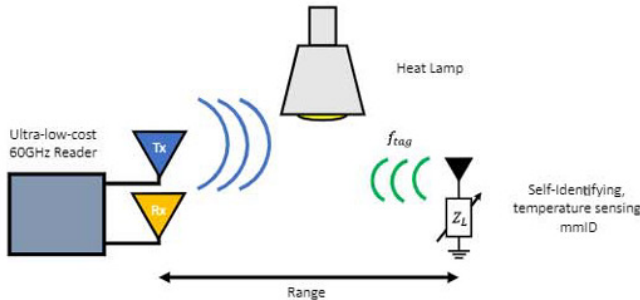


Figure 11: Diagram of the top view local temperature monitoring scenario of single mmID.

each step. In Fig. 12, one can view the estimated range of the mmID with the change in instantaneous frequency of the mmID due to changes in the local temperature. With a maximum average ranging error of 5.35 mm, the self-identifying mmID enables precise ranging of local temperature.

B. Simultaneous Multi-tag Interrogation

Having designed and characterized a single temperature sensing mmID, another mmID was fabricated using the same system components. The gain resistors of the differential amplifier circuit was adjusted in order to provide a unique identification frequency. Having these two proof-of-concept, self-identifying temperature sensing mmIDs, multi-tag interrogation was enabled. In Figure 13, one can view the three configurations of the temperature sensing mmIDs namely, both mmIDs subject to ambient temperature without heating, focusing the heat of the lamp on each tag separately. The

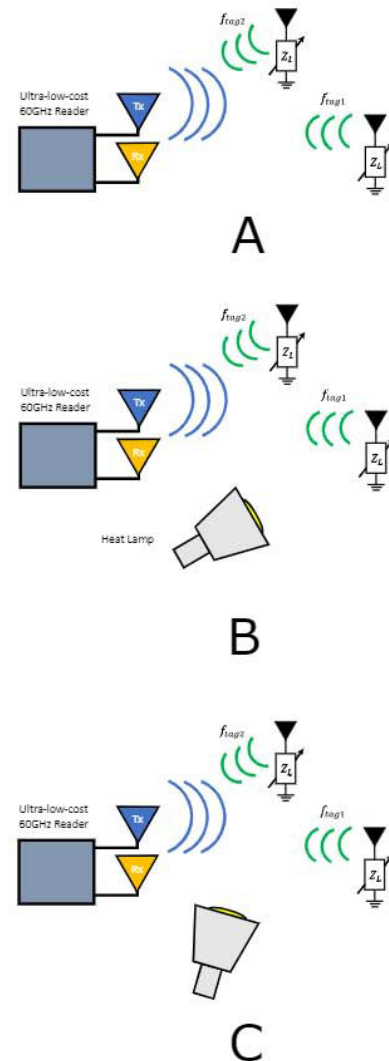


Figure 13: Multi-tag interrogation schematics.

tracking of range, and focusing the heat on each tag with

the mmIDs stationary throughout the measurements. During each scenario, the ranging, 2D AoA estimation, and local temperature of each mmID were recorded and are displayed in Table II.

Table II: Statistics of range, AoA, and local temperature of each self-identifying mmID for the multi-tag interrogation scenarios where * and ** denote $mmID_1$ and $mmID_2$, respectively.

Scenario	Range (cm)	AoA (°)	Local Temp. mmmID (°C)
A	40.49*/28.10**	0.0*/-12.46**	24.00*/24.00**
B	40.52*/28.10**	0.0*/-10.08**	33.78*/26.265**
C	40.49*/28.19**	0.0*/-13.55**	25.20*/28.98**

These recorded statistics highlight the ability of the 'Smart' packaged, self-identifying, temperature sensing mmID system enable fine localization and digital twinning of temperature gradient environments in close proximity to each other.

V. CONCLUSION

In this work, the authors present a "Smart" packaging of self-identifying and localizable mmID system for temperature sensing applications. The proposed system leveraged the usage of additive manufacturing technologies in order to realize the ultra-low-cost, scalable mmID front-end and sensor element. The mmID itself is surface agnostic and designed on flexible substrate providing a sticker-like form-factor for digital twinning applications. Lastly, the authors presented a simultaneous interrogation of two mmIDs in close proximity to each other. Thus, enabling a framework for interrogation of dense population of self-identifying sensing mmID's in an environment to act as a digital twin in smart city and smart home applications.

ACKNOWLEDGMENT

The authors would like to acknowledge the support of the National Science Foundation and the Air Force Office of Scientific Research.

REFERENCES

[1] R. Bhattacharyya, C. Floerkemeier, S. Sarma, and D. Deavours, "Rfid tag antenna based temperature sensing in the frequency domain," in *2011 IEEE International Conference on RFID*, 2011, pp. 70–77.

[2] J. G. Hester and M. M. Tentzeris, "A mm-wave ultra-long-range energy-autonomous printed rfid-enabled van-atta wireless sensor: At the crossroads of 5g and iot," in *2017 IEEE MTT-S International Microwave Symposium (IMS)*, 2017, pp. 1557–1560.

[3] D. Henry, J. G. D. Hester, H. Aubert, P. Pons, and M. M. Tentzeris, "Long range wireless interrogation of passive humidity sensors using van-atta cross-polarization effect and 3d beam scanning analysis," in *2017 IEEE MTT-S International Microwave Symposium (IMS)*, 2017, pp. 816–819.

[4] A. Adeyeye, C. Lynch, X. He, S. Lee, J. D. Cressler, and M. M. Tentzeris, "Fully inkjet printed 60ghz backscatter 5g rfid modules for sensing and localization in internet of things (iot) and digital twins applications," in *2021 IEEE 71st Electronic Components and Technology Conference (ECTC)*, 2021, pp. 1193–1198.

[5] R. A. Bahr, A. O. Adeyeye, S. Van Rijs, and M. M. Tentzeris, "3d-printed omnidirectional luneburg lens retroreflectors for low-cost mm-wave positioning," in *2020 IEEE International Conference on RFID (RFID)*, 2020, pp. 1–7.

[6] X. He, B. K. Tehrani, R. Bahr, W. Su, and M. M. Tentzeris, "Additively manufactured mm-wave multichip modules with fully printed "smart" encapsulation structures," *IEEE Transactions on Microwave Theory and Techniques*, vol. 68, no. 7, pp. 2716–2724, 2020.

[7] C. A. Lynch, A. O. Adeyeye, J. G. Hester, and M. M. Tentzeris, "When a single chip becomes the rfid reader: An ultra-low-cost 60 ghz reader and mmid system for ultra-accurate 2d microlocalization," in *2021 IEEE International Conference on RFID (RFID)*, 2021, pp. 1–8.